Investigating the association of electrically-evoked compound action potential thresholds with inner-ear dimensions in pediatric cochlear implantation

Söderqvist, Samuel

2022-07

Söderqvist , S , Sivonen , V , Lamminmäki , S , Ylönen , J , Markkola , A & Sinkkonen , S T 2022 , ' Investigating the association of electrically-evoked compound action potential thresholds with inner-ear dimensions in pediatric cochlear implantation ' , International Journal of Pediatric Otorhinolaryngology , vol. 158 , 111160 . https://doi.org/10.1016/j.ijporl.2022.111160

http://hdl.handle.net/10138/345945
https://doi.org/10.1016/j.ijporl.2022.111160

International Journal of Pediatric Otorhinolaryngology 158 (2022) 111160

Contents lists available at ScienceDirect

International Journal of Pediatric Otorhinolaryngology

journal homepage: www.elsevier.com/locate/ijporl

Investigating the association of electrically-evoked compound action potential thresholds with inner-ear dimensions in pediatric cochlear implantation

Samuel Söderqvist [a,*], Ville Sivonen [a], Satu Lamminmäki [a], Jere Ylönen [a,b], Antti Markkola [c], Saku T. Sinkkonen [a]

[a] Department of Otorhinolaryngology – Head and Neck Surgery, Head and Neck Center, Helsinki University Hospital and University of Helsinki, Helsinki, Finland
[b] Department of Otorhinolaryngology, Päijät-Häme Central Hospital, Päijät-Häme Joint Authority for Health and Wellbeing, Finland
[c] Department of Radiology, Helsinki University Hospital and University of Helsinki, Helsinki, Finland

ARTICLE INFO

Keywords:
Cochlear implant
Electrically-evoked compound action potential
Cochlea diameter
Cochlear nerve
Inner ear dimension

ABSTRACT

Objectives: A narrow bony cochlear nerve canal (BCNC), as well as a hypoplastic and aplastic cochlear nerve (CN) have been associated with increased electrically-evoked compound action potential (eCAP) thresholds in some studies, suggesting poorer neural excitability in cochlear implantation. Also, in large cochleae the extent of activated spiral ganglion neurons with electrical stimulation is less than in smaller ones. However, a detailed description of the relationship between eCAP thresholds for a lateral-wall electrode array and dimensions of the inner-ear structures and internal auditory canal (IAC) is missing.

Design: The study subjects were 52 pediatric patients with congenital severe-to-profound hearing loss (27 females and 25 males; ages 0.7–2.0 years; 1.0 ± 0.3 years, mean ± SD) implanted bilaterally with Cochlear Nucleus CI422, CI522, or CI622 implants with full insertion of the Slim Straight electrode array. Diameters of the cochlea and the BCNC as well as the widths and heights of the IAC and the CN were evaluated from preoperative computed tomography and magnetic resonance images. These anatomical dimensions were compared with each other and with the patients' intraoperative eCAP thresholds.

Results: The eCAP thresholds increased from the apical to basal direction ($r = 0.89$, $p < 0.001$). After sorting the cochleae into four size categories, higher eCAP thresholds were found in larger than in smaller cochleae ($p < 0.001$). With similar categorization, the eCAP thresholds were higher in cochleae with a larger BCNC than in cochleae with a smaller BCNC ($p < 0.001$). Neither IAC nor CN cross-sectional areas affected the eCAP thresholds. Correlations were found between cochlea and BCNC diameters and between IAC and CN cross-sectional areas ($r = 0.39$ and $r = 0.48$, respectively, $p < 0.001$ for both).

Conclusions: In the basal part of the electrode array, higher stimulation levels to elicit measurable neural responses (eCAP thresholds) were required than in the apical part. Increased eCAP thresholds associated with a larger cochlear diameter, but contrary to the earlier studies, not with a small size of the BCNC or the CN. Instead, the BCNC diameter correlated significantly with the cochlea diameter.

1. Introduction

A cochlear implant (CI) is a neuroprothesis that helps to perceive sound and promotes language development in severely hearing-impaired children [1]. With a CI, the structures of the external and the middle ear as well as the non-functioning hair cells of the organ of Corti in the inner ear are surpassed, and auditory sensation is elicited by directly stimulating the spiral ganglion neurons (SGN). The SGN axons exit the cochlea at the modiolus and form the cochlear nerve (CN) bundle in the bony cochlear nerve canal (BCNC). From the BCNC, the CN accesses the internal auditory canal (IAC) on its way to the cochlear nucleus. As physiology relies on anatomy, malformations of the inner ear can affect auditory processing and therefore hearing outcomes [2–5].

* All Correspondence should be addressed to: Department of Otorhinolaryngology – Head and Neck Surgery, Helsinki University Hospital, Kasarmikatu 11-13, 00130, Helsinki, Finland.
E-mail address: sachso@utu.fi (S. Söderqvist).

https://doi.org/10.1016/j.ijporl.2022.111160
Received 29 November 2021; Received in revised form 12 March 2022; Accepted 23 April 2022
Available online 26 April 2022

The activation of the SGNs in CI users can be investigated by measuring the electrically-evoked compound action potential (eCAP), which also provides an objective verification of the CI device function. A typical eCAP response is biphasic in morphology, consisting of a negative and a positive peak [6]. Sometimes the eCAP also shows a second positive peak which is thought to reflect late dendritic activation of the SGNs. The eCAP amplitude is defined as the difference between the negative and positive peaks in microvolts (μV), and depicts the strength and synchrony of the SGN activation [6]. As the eCAP amplitude increases with the stimulation current, the responsiveness of the auditory nerve can be evaluated via the slope of the eCAP amplitude growth function (AGF; [7]). The AGF can be extrapolated to estimate the eCAP threshold, which is the smallest electrical current that produces an eCAP amplitude of zero. A low eCAP threshold indicates that the CN is easily excitable with electrical stimulation. However, even though the eCAP threshold is thought to reflect neural health, it seems to have only a weak to moderate correlation with the behavioral stimulation levels [8, 9].

Many malformations of the inner ear have been associated with abnormalities in eCAP measurements. Cochleae with a stenotic BCNC, defined to be under 1.5 mm in diameter, display higher eCAP thresholds when compared to cochleae with a wider BCNC [10]. Jang et al. [11] showed an inverse correlation of the eCAP thresholds with both the BCNC diameter and the CN cross-sectional area for a few individual electrodes in the basal section of the electrode array. In addition, in ears with a small CN, the eCAP thresholds were higher when the BCNC was narrow (below-average) in comparison to patients with a wide (above-average) BCNC [11]. These data suggest that small BCNC dimensions are associated with higher eCAP thresholds. However, Han et al. [10] did not report the type or manufacturer of the electrode arrays used in the study, and the study of Jang et al. [11] included both perimodiolar and lateral-wall electrode arrays.

Cochleae with hypoplastic and aplastic CNs have higher eCAP thresholds and shallower AGF slopes when compared to normal [12]. In He et al. [12], the CN was qualified to be hypoplastic if it was smaller in an MRI than the other nerves in the IAC or than the contralateral CN, and aplastic if it was unidentifiable. However, when the CN is normal, the diameter of the CN and the eCAP thresholds show no correlation [13].

To summarize, the effects of BCNC diameter and CN size on eCAP thresholds have been explored in earlier studies. However, the dimensions of the inner-ear structures might correlate with each other and thus form a confounding factor. Cochlea diameter shows a weak-to-moderate correlation with the extent of activated SGNs (spread of excitation; [14]) and therefore, it affects the neural responsiveness of the cochlea. In this study, correlations between the dimensions of the cochlea, the BCNC, the IAC, and the CN were evaluated, and then compared with the intraoperative eCAP thresholds of a lateral-wall electrode array. As the angular insertion depth of the electrode array affects eCAP thresholds [15], the location of each electrode contact was evaluated as a linear electrode number on the array and as an estimated insertion angle. As the age and the duration of pre-implantation hearing loss might also affect the SGN density and eCAP thresholds [16], we investigated only congenitally hearing-impaired children implanted before the age of two years. Our hypothesis was that the eCAP thresholds of a lateral-wall electrode array are elevated in ears with a large cochlea and in ears with a small BCNC, IAC, or CN.

2. Materials and methods

2.1. Study design and ethics

This was a retrospective cohort study approved by the institutional review board of the Hospital District of Helsinki and Uusimaa. Due to the retrospective nature of the study, the ethical committee and informed consent were not required by the Finnish national legislation.

2.2. Subjects

The subjects included in the study were pediatric patients with congenital severe-to-profound hearing loss implanted bilaterally before the age of two with Cochlear Nucleus CI422, CI522, or CI622 implants (Cochlear Ltd, Sydney, Australia) with the Slim Straight electrode arrays between December 2011 and November 2020 at Helsinki University Hospital at the Department of Otorhinolaryngology – Head and Neck Surgery. No patients were excluded from the study due to incomplete insertion of the electrode array, as according to the patients' operative reports, the electrode arrays were completely inserted inside the cochleae in all patients.

2.3. eCAP thresholds

The eCAP thresholds and amplitudes were recorded via neural response telemetry (NRT) and measured with Custom Sound EP software (Cochlear Ltd, Sydney, Australia) during the final stage of the CI surgery when the patient was still under general anesthesia. To record NRT, a pulse width of 25 μs and a rate of 250 Hz was used, which is the default setting. The eCAP thresholds were automatically determined by the recording software. Out of the 104 ears, the eCAP thresholds were not recorded for 5 ears. For each individual electrode contact, the eCAP threshold of minimum 68 ears were available. The eCAP thresholds are shown in detail in Table 1 in Appendix.

2.4. Anatomical dimensions

All patients were preoperatively imaged with a high-resolution computed tomography (CT) and an MRI using a standard clinical protocol used in the Hospital District of Helsinki and Uusimaa. The CT scans were performed in a supine position using multidetector CT scanners (GE LightSpeed VCT and GE Revolution, GE Healthcare, Milwaukee, WI, USA). The slice thickness of the reconstructed CT images was 0.31–0.63 mm. The preoperative MRI scans were performed using either 1.5 or 3.0 T MRI scanners (Philips Achieva and Philips Ingenia, Philips Medical Systems, Nederland). The native scans included axial T2-weighted images covering the whole brain (slice thickness 3.0 mm) and 3D axial T2-weighted images covering the temporal bones (the slice thickness of the reconstructed parasagittal oblique image 0.58–1.00 mm).

The diameter of the cochlea was evaluated by an otoradiologist from the reconstructed CT images of the cochlea as described by Alexiades et al. [17]. Two trained medical doctors evaluated the diameter of the BCNC and the width of the IAC from the axial CT image, the height of the IAC from the coronal CT image, and the width and the height of the CN from a reconstructed parasagittal oblique MRI image as described in Chetcuti and Kumbla [18]. The images were evaluated with a digital measurement tool with a resolution of 0.1 mm. Fig. 1 illustrates the measurements in more detail. The estimations of the IAC and the CN cross-sectional areas were derived from multiplying the corresponding height with the width as described by Herman and Angeli [19]. Out of the 104 ears, information about the cochlea diameter, the IAC height and width, and the CN height and width were unavailable for 3, 1, and 8 ears, respectively.

2.5. Electrode insertion angle

To confirm of the analysis about the effect of electrode location, computational electrode insertion angles were applied in addition to the actual electrode numbers. Based on the patients' operative charts, all the CI electrode arrays were fully inserted through the round window route. The most basal electrode is located 5 mm from the full insertion mark along the Slim Straight electrode array. The following 21 electrodes are spread across 19.1 mm in the active part of electrode array, leading to a distance of 0.91 mm between the electrodes. Therefore, the linear location of each electrode's basal edge (L in mm) was calculated using:

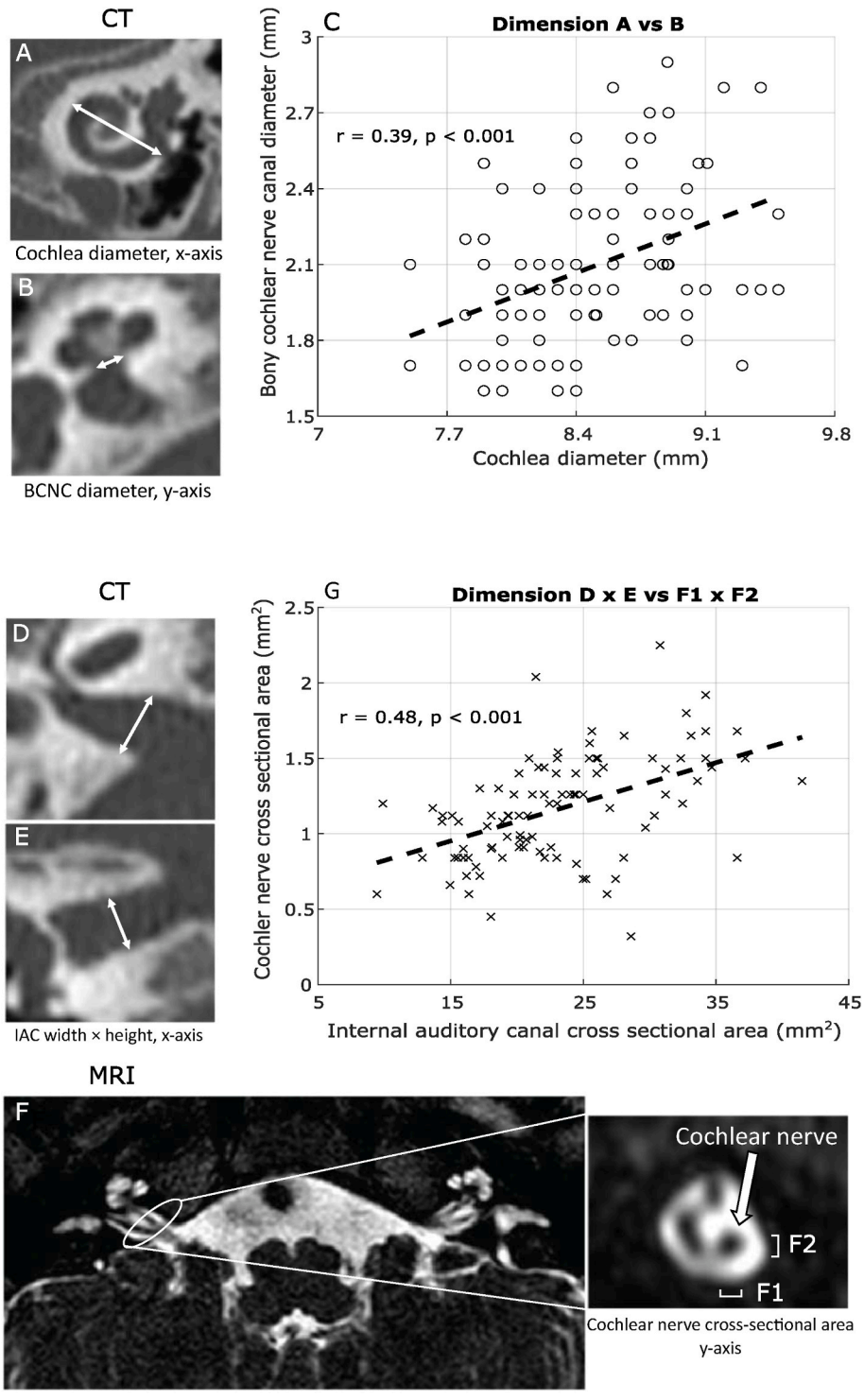

Fig. 1. Inner-ear and IAC dimensions and correlations. Representative computed tomography (CT; A, B, D, and E.) and magnetic resonance image (MRI, F.) scans. The white lines demonstrate corresponding measurement: **A.** cochlea diameter from a reconstructed CT image, **B.** bony cochlear nerve canal diameter from an axial CT, **D.** width and **E.** height of internal acoustic canal from axial and coronal CT scans, respectively, and **F.** cochlear nerve height (F1) and width (F2) from a parasagittal oblique MRI. Significant correlations after Bonferroni correction were detected between the cochlear diameter and the bony cochlear nerve canal (BCNC) diameter (**C**, Pearson's r = 0.39, $p < 0.001$), and between the cross-sectional areas of the IAC and the cochlear nerve (**G**, r = 0.48, $p < 0.001$).

$$L = 5.0 + 0.91 \times (electrode\ number - 1)\ mm$$

Each electrode was assumed to lie next to the lateral wall and Equation (3) in Escudé et al. [20] was applied to estimate an individual insertion angle:

$$Insertion\ angle = (\exp(L \div (cochlea\ diameter \times 2.62)) - 1) \times 235\ degrees.$$

The insertion angle range was 52–68 and 380–570°, and the mean insertion angle ± SD was 59 ± 3.5 and 460 ± 40°, for the most basal and apical electrodes, respectively.

2.6. Statistics

For statistical analysis, the ears were sorted into four groups according to the distributions of their anatomical dimensions. The mean ± SD for the cochlea diameter was 8.50 ± 0.45 and for the BCNC diameter 2.10 ± 0.31 mm. The mean ± SD for the IAC and the CN cross-sectional areas were 23.0 ± 6.52 and 1.05 ± 0.33 mm^2, respectively. In the first group, the dimensions are less than −1 SD, in the second group between −1 SD and the mean, in the third group between the mean and 1 SD, and in the fourth group larger than 1 SD, resulting in 18, 35, 31, and 17 ears

in the corresponding groups for the cochlea. For the BCNC, the respective number of ears in each group were 17, 35, 36, and 16; for the IAC 18, 37, 28, and 19 ears; and for the CN 14, 36, 31, and 15 ears. Also, the insertion depths were divided into 20 categories. The lower limit of the first category was 50° and the spacing between each category was 25°. As an exception, to reach a sufficient number of subjects, the width of the last category was increased to 45° with the upper limit of 570°. The eCAP measurements and the inner-ear dimensions were analyzed statistically with IBM SPSS 25 (IMB, Armonk, New York) using a two-way analysis of variance (ANOVA) with cochlea diameter group and electrode contact or insertion angle category as independent variables and eCAP threshold as a dependent variable. The p-values in post-hoc analyses were corrected with the Tukey method. The correlation coefficients (Pearson's *r*) were computed between the different anatomical dimensions and between the electrophysiological measurements and the location along the electrode array, defined either as electrode contact or insertion angle.

3. Results

In this study, we investigated the effect of the inner-ear dimensions on eCAP thresholds. A total of 52 patients (27 females and 25 males; ages 0.7–2.0 years; 1.0 ± 0.3 years, mean ± SD) were included in the study. The etiologies of hearing loss were mutation in the Connexin 26 gene (n = 23), maternal CMV infection during pregnancy (n = 3), a long QT syndrome (n = 1), and unknown (n = 25).

Fig. 1 demonstrates the measured inner-ear dimensions and correlations between different dimensions. The cochlea and BCNC diameters are shown in Fig. 1A and B, the IAC width and height in Fig. 1D and E, and the CN cross-sectional area in Fig. 1F. Significant correlations after Bonferroni corrections were found between the cochlea and the BCNC diameters (Fig. 1C; $r = 0.39$, $p < 0.001$) and between the cross-sectional areas of the IAC and the CN (Fig. 1G; $r = 0.48$, $p < 0.001$). Either the cochlea or the BCNC diameter showed no significant correlation with the IAC or the CN cross-sectional area.

Fig. 2 shows the mean eCAP thresholds along the electrode array, which are arranged from the apex (electrode 22) to the base (electrode 1). As seen in Fig. 2A, the mean eCAP thresholds increase from apical to basal direction ($r = 0.89$, $p < 0.001$), demonstrating that less current is needed to elicit an eCAP response in the apex than in the middle or in the basal parts of the electrode array. However, the relationship between the eCAP threshold and the electrode contact is non-monotonic and non-linear, and therefore, a fifth order polynomial was fitted to the data. The correlation coefficient between the polynomial and the mean data was 0.97, and the corresponding 95% confidence intervals of the polynomial fit are plotted in Fig. 2A. In Fig. 2B, the mean eCAP thresholds are presented in a heatmap. When the patients were divided into four groups according to their cochlea diameter (Fig. 2C), a two-way ANOVA revealed significant main effects of cochlea diameter group and electrode contact ($F(3, 1758) = 28.2$ and $F(21,1758) = 22.1$, $p < 0.001$ for both). Their interaction was not significant ($F(63,1758) = 1.25$, $p = 0.09$). The mean eCAP thresholds were significantly lower in the first two groups with the smallest cochleae than in the rest of the groups (185 current level (CL) in both vs. 193 and 190 CL, respectively, $p < 0.001$ for all). Altogether these results suggest that the eCAP threshold is lower in smaller dimensions (i.e. either a more apical electrode contact location or a smaller cochlea).

As the cochlea diameter affects the insertion depth and angle of the array [20] and the insertion angle affects the eCAP thresholds [15], we wanted to minimize this effect by calculating the insertion angle of the individual electrodes for further analysis. As illustrated in Fig. 2D, when the locations of the electrodes were assessed via insertion angles, the correlation between the polynomial and the mean data was slightly higher 0.98 with narrower 95% confidence intervals when compared to Fig. 2A. Fig. 2E depicts the mean eCAP threshold as a function of insertion angle category and shows a smoother heatmap than Fig. 2B. Further, to evaluate the effect of cochlea diameter on eCAP thresholds in different insertion angles, the patients were divided into the same cochlea diameter groups as with the electrode contacts (Fig. 2F). The five largest insertion angle categories were left out from further statistical analysis, as the electrode array does not reach these insertion angles in the larger cochleae. Significant main effects of cochlea diameter group

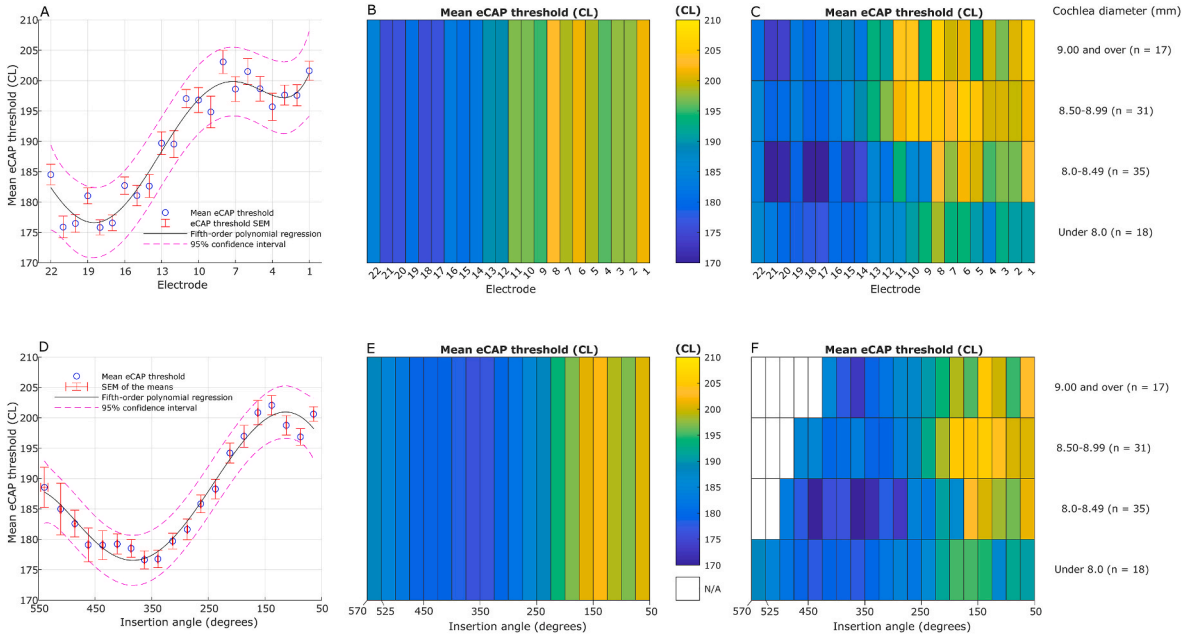

Fig. 2. The mean eCAP thresholds at individual locations and cochlea diameters. In each plot, the individual electrode contacts are arranged from apical to basal direction. **A. and D.** The mean ± standard error of the mean (SEM) eCAP threshold is plotted at individual (A) electrode contacts and (D) mean insertion angle of each category. The respective fitted fifth-order polynomial have correlations of 0.97 and 0.98 with the measurement data. **B and E.** The mean eCAP thresholds at individual electrode contacts and insertion angles. **C and F.** The eCAP thresholds at individual electrode contacts and insertion angles are grouped by cochlea diameter. The largest cochleae maximum insertion depth did not reach the limits of largest insertion angles (F, white cells in upper left corner).

and insertion angle category were found ($F(3,1578) = 13.9$, $p < 0.001$ and $F(14,1578) = 25.4$, $p < 0.001$, respectively), indicating that when accounting for the dependence of the longitudinal location of an electrode contact on the cochlear size, the mean eCAP thresholds are still associated with the cochlea diameter. No significant interaction between cochlea diameter group and insertion angle category were detected ($F(42,1578) = 1.2$, $p = 0.22$). Similarly as earlier, the mean eCAP thresholds were significantly lower in the two groups of the smallest cochleae than in the rest of the groups (187 in both vs. 193 and 190 CL, respectively, $p < 0.05$ for all).

Fig. 3 shows the mean eCAP thresholds along the electrode array in the cochleae grouped by the BCNC diameter, similarly as with the cochlea diameter in Fig. 2. When the effect of the BCNC diameter and the insertion angle on the eCAP thresholds was analyzed, main effects of BCNC diameter group and insertion angle category were found ($F(3, 1607) = 8.76$ and $F(14, 1607) = 24.5$, $p < 0.001$ for both). Further, the eCAP thresholds were compared with the dimensions of anatomical structures outside the cochlea, and the cochleae were grouped based on their IAC and CN cross-sectional areas. When the effect of the groups on the eCAP thresholds were analyzed in the different insertion angles, only a significant main effect of insertion angle category was found ($F(14,1600) = 26.5$ and $F(14,1497) = 23.60$, respectively, $p < 0.001$ for both).

4. Discussion

The aim of the present study was to investigate the relationship between inner-ear dimensions and electrophysiology via eCAP measurements in congenitally severely-to-profoundly hearing-impaired patients implanted with CIs under the age of two years. As our cohort contains patients with normally sized structures, our results might be helpful in determining the initial stimulation levels used in intraoperative eCAP recordings and post-operative adjustments of the CI in the majority of patients.

The results suggest that eCAP thresholds are generally higher in larger cochleae than in smaller ones. When the electrode array is fully inserted, the maximum insertion depth is greater in small cochleae when compared to larger cochleae, as the electrode array used in this study lies supposedly next to the lateral wall. Therefore, to minimize the effect of cochlea diameter on the electrode location inside the cochlea, the insertion angle was calculated for each electrode contact in each cochlea. However, even after this adjustment, larger cochleae had higher eCAP thresholds than smaller ones in the corresponding insertion angles, so the different angular location of the electrode contacts do not explain these results alone. As the perpendicular measurement of the cochlea diameter increases with the cochlea size [20], also the volume of the cochlear duct increases with the height and width of the scala tympani (ST; [21]). The greater cross-sectional area of the ST leads to a larger modiolar distance, which provides an additional explanation for the elevated eCAP thresholds in large cochleae [22–24]. In this study, the maximum diameter difference between the smallest and largest cochleae was 2 mm, and with a rough estimation, the modiolar distance is approximately 1 mm greater in the former than in the latter, assuming that the electrode is next to the lateral wall. An earlier study [23] found that the minimum current must be increased with approximately 25% per 1 mm increase in modiolar distance to elicit an auditory sensation (2 dB in electrical current per mm in monopolar stimulation). In our study, when the eCAP threshold was converted to mA, as the CL is an exponential unit, the difference was approximately 15% per mm when computed over all the cochleae and the electrode contacts between the insertion angles from 50 to 450°. However, Long et al. [23] used a perimodiolar electrode array with postoperative imaging and therefore, included a more accurate assessment of the modiolar distance than what was estimated in our study based on the assumption that the electrode array resides next to the lateral wall and modiolar distance was approximated only based on the diameter of the cochlea.

As seen in Fig. 2F, the differences in the eCAP thresholds between the smallest and largest cochleae seem to even out at around an insertion angle of 250°, where the cross-sectional diameter of the ST [25] and the modiolar distance [26] decreases rapidly. These results suggest that the eCAP thresholds increase with modiolar distance. However, post-operative CT imaging is not a routine in our clinic, as abnormal findings are rare [27] and anesthesia is required in pediatric patients. Therefore, the exact placement of the electrode array is unknown, and the cochlea diameter might have additional effects on eCAP thresholds. In our earlier study we speculated, that the electrode-generated charge density might be decreased in large cochleae, and therefore higher stimulation is needed to get a neural response [14]. In addition, the sensitivity of eCAP measurement might decrease with the increasing modiolar distance, because the potential difference caused by the neural excitation is likely to weaken before encountering the recording electrode, leading to erroneously high thresholds.

Contrary to earlier studies, we found higher eCAP thresholds in cochleae with larger BCNC than in cochleae with smaller BCNC. In earlier studies, cochleae with a stenotic BCNC have been reported to have higher eCAP thresholds in the apical and basal sections of the electrode array when compared to cochleae with a normal BCNC [10]. Jang et al. [11] found an inverse correlation between the BCNC diameter and the eCAP threshold in the basal section of the electrode array. However, as the diameters of the cochlea and BCNC correlate in our study sample (Fig. 1), the higher of eCAP thresholds in cochleae with larger BCNCs are probably due to the increased cochlea diameter and

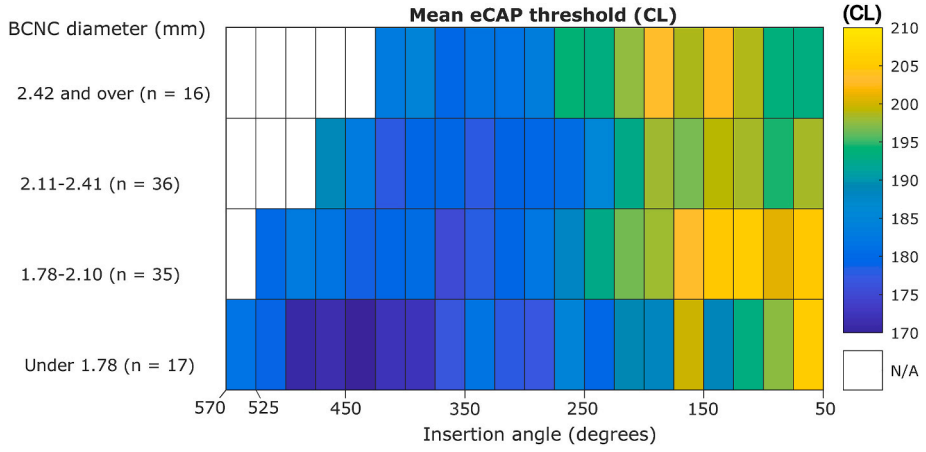

Fig. 3. Mean eCAP thresholds grouped by bony cochlear nerve canal diameter (BCNC). The individual insertion angles are arranged from apical to basal direction. The largest cochleae maximum insertion depth did not reach the limits of largest insertion angles (B, white cells in upper left corner).

modiolar distance. Even though there was a great intersubject variability between the BCNC diameters in our study population, the smallest BCNC diameter was 1.60 mm, which is not considered stenotic. Therefore, the BCNC diameter possibly affects eCAP thresholds only under a certain cut-off diameter.

In our study, the mean CN cross-sectional area was similar as in normal-hearing population [19,28] and larger than in post-lingually deafened patients [19]. In agreement with an earlier study [13], the eCAP thresholds were not affected by the CN cross-sectional area in the normal CN. These results suggest, similarly with the BCNC, that the CN has an effect on the eCAP thresholds only when it is abnormally small or absent [12]. This study population included no patients with aplastic or hypoplastic CN, but in future it would be valuable to investigate eCAP thresholds in different kind of anomaly ears because earlier studies show that the hearing rehabilitation results are highly variable and generally worse in ears with CN hypoplasia when compared to normal [29,30]. In CI recipients with CN aplasia the hearing outcomes are even worse, 65% of the patients use sign language as their main mode of communication [30].

In line with the earlier studies of lateral-wall electrode arrays [31–33], this study demonstrates that the eCAP thresholds increase from apical to basal direction. This is illustrated in an anatomical sketch of Fig. 4. In the most apical insertion angles, however, there are increases in the eCAP thresholds. The increases could be explained with the measurement method, where the eCAP recording electrode is usually two electrodes to the apical direction of the stimulating electrode. However, in the apical end the recording location is two electrodes basal to the stimulating electrode potentially leading to unrealistically high eCAP thresholds, as it is affected by both the masker and probe amplitudes [6]. Also, the tilted 'S'-shape of the fitted mean eCAP threshold polynomial in the base, which could be due to the varying modiolar distance before the array reaches the lateral wall [34].

The modeled insertion angles in this study seem realistic, when compared to the measured mean and maximum insertion angles for the same electrode array [34]. Also, even though the whole length of the cochlear duct might not be predictable from the cochlea diameter, the latter and the two-turn length have a strong correlation [35], further confirming the validity of our insertion angle estimation. However, as the electrode array used in this study reaches the lateral wall approximately at an insertion angle of 90° [34], the modeled insertion angle of the few first basal electrodes is probably inaccurate, and could have repercussions for the rest of the electrode array. Also, eCAP thresholds are higher when the electrode array is placed in the scala vestibuli when compared to the placement in the ST [15]. Without post-operative imaging, the scalar location of individual electrodes cannot be evaluated. However, when the Slim Straight electrode array is implanted using the round window approach, the rate of scalar change (i.e. the placement of the electrode array is in the scala vestibuli instead of the ST) is low [36].

Another limitation of this study is the possibility of measurement error due to the relatively low resolution of the CT and MRI images when compared to the small dimensions of the measured structures. Even though previously a good interobserver correlation for calculating cross-sectional areas from parasagittal MRIs have been reported [28] and our measurements were partially cross-checked, three observers increases the risk of measurement error. However, the images were taken with state-of-the-art clinical CT and MRI machines, and postprocessed and analyzed with qualified methods broadly used in clinical settings. Finally, even though the patient cohort includes all congenitally severely-to-profoundly hearing-impaired patients implanted bilaterally in our unit with this electrode type during the study period, the sample size is relatively low. Thus, further studies with larger cohorts are warranted.

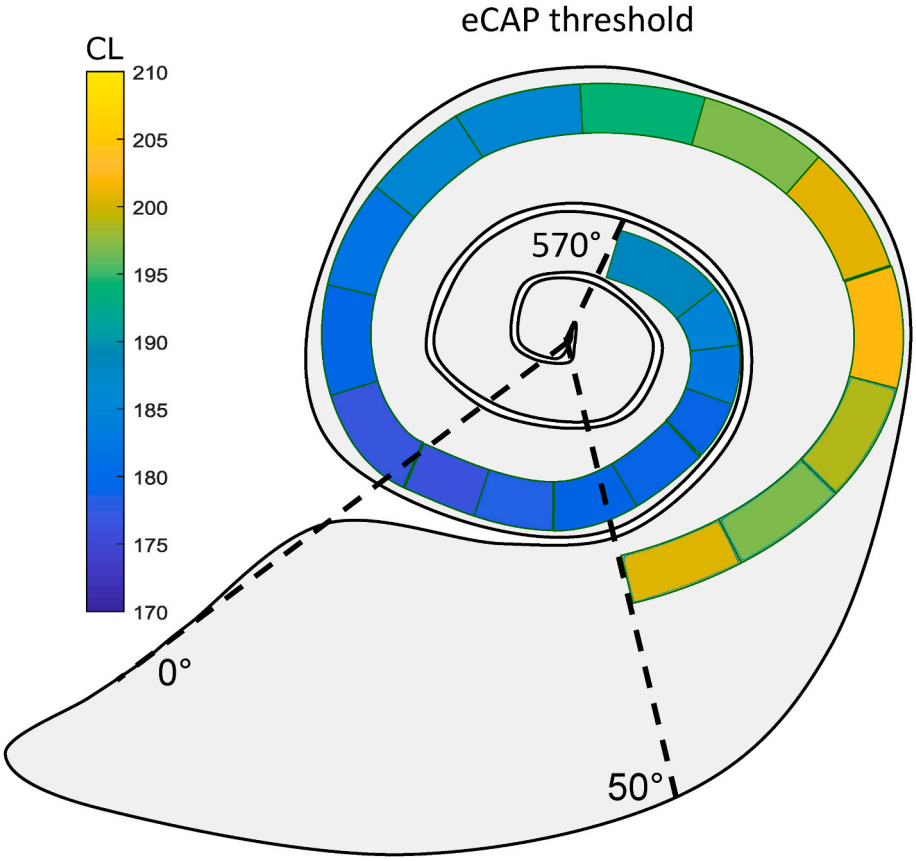

Fig. 4. The mean eCAP thresholds in the scala tympani. In complete insertion, the linear distance of the most basal electrode is 5 mm from the round window. The insertion angle range is 50–570° and each cell covers 25°, with the exception of the most apical cell, which covers 45°.

5. Conclusion

The eCAP thresholds increased from apical to basal direction along the lateral-wall electrode array and higher eCAP thresholds were found in larger than in smaller cochleae. As scala tympani cross-sectional area is dependent on the location along the cochlear turns and affected by cochlea size, this suggests that eCAP thresholds are dependent on the cross-sectional area of the scala at the electrode contact site. Since the cochlea diameter correlated with the diameter of the BCNC, our results were in contrast with earlier studies reporting elevated eCAP thresholds in cochleae with small BCNCs. In this study sample, neither the cross-sectional area of the IAC nor CN affected the eCAP thresholds.

Conflicts of interest and source of funding

There are no conflicts of interest, financial, or otherwise.

Declarations of competing interest

None.

Acknowledgements

This research did not receive any specific grant from funding agencies in the public, commercial, or not-for-profit sectors.

Appendix

Table 1
The cochlea and BCNC diameters (Ø), IAC and CN cross-sectional areas (CSA), and eCAP thresholds.

Ear	Cochlea Ø (mm)	BCNC Ø (mm)	CN CSA (mm^2)	IAC CSA (mm^2)	eCAP threshold (CL)								
					22	21	20	19	18	17	16	15	14
1L	9.4	2.0	1.1	22.1	180	N/A	N/A	187	N/A	N/A	180	N/A	N/A
1R	N/A	2.0	0.8	24.5	174	N/A	N/A	174	N/A	N/A	178	N/A	N/A
2L	N/A	2.4	1.1	21.6	195	173	172	186	172	179	192	192	184
2R	8.6	2.0	1.4	34.7	198	N/A	N/A	194	N/A	N/A	182	N/A	N/A
3L	8.6	2.8	1.4	26.5	192	187	186	185	181	181	187	185	187
3R	7.9	2.5	1.3	25.7	171	N/A	N/A	167	N/A	N/A	160	N/A	N/A
4L	8.0	2.0	0.5	15.5	N/A	N/A	N/A	N/A	N/A	N/A	N/A	N/A	N/A
4R	8.0	1.6	0.3	18.0	N/A	N/A	N/A	N/A	N/A	N/A	N/A	N/A	N/A
5L	8.6	2.3	1.0	34.2	180	N/A	N/A	164	N/A	N/A	188	N/A	N/A
5R	8.4	2.0	0.8	28.1	192	N/A	N/A	183	N/A	N/A	184	N/A	N/A
6L	8.4	2.1	0.6	22.1	186	N/A	N/A	190	N/A	N/A	187	N/A	N/A
6R	8.7	2.5	0.7	24.0	207	190	195	192	184	191	198	200	201
7L	8.1	2.0	1.0	20.2	165	N/A	N/A	N/A	N/A	N/A	176	N/A	N/A
7R	8.4	2.6	N/A	16.9	189	N/A	N/A	205	N/A	N/A	196	N/A	N/A
8L	9.4	2.8	1.1	26.1	192	N/A	N/A	185	N/A	N/A	194	N/A	N/A
8R	9.0	2.3	0.8	20.2	186	N/A	N/A	185	N/A	N/A	188	N/A	N/A
9L	8.2	2.0	0.8	19.4	180	173	182	176	178	179	188	183	189
9R	8.8	2.6	1.1	17.8	N/A	N/A	N/A	N/A	N/A	N/A	N/A	N/A	N/A
10L	8.1	1.9	1.1	34.2	189	150	N/A	174	174	165	171	150	165
10R	9.0	1.9	1.1	23.0	204	199	198	197	N/A	191	200	203	204
11L	8.5	2.3	1.0	19.8	201	203	196	202	194	190	188	192	194
11R	8.2	1.8	0.8	19.3	180	167	169	179	169	163	175	165	171
12L	8.9	2.7	0.8	23.0	171	170	174	169	170	170	183	184	189
12R	8.2	2.1	1.1	41.5	210	N/A	N/A	222	N/A	N/A	207	N/A	N/A
13L	8.3	2.1	1.4	30.2	204	N/A	N/A	202	N/A	N/A	205	N/A	N/A
13R	8.3	1.7	0.6	16.4	186	172	173	173	173	170	176	181	185
14L	7.5	1.7	1.5	32.8	192	184	180	177	178	177	189	179	178
14R	8.1	2.1	N/A	N/A	168	184	180	181	173	174	169	176	176
15L	8.8	2.3	0.6	9.5	198	191	187	198	189	190	203	201	204
15R	7.9	1.7	0.8	12.9	201	174	169	191	176	176	204	184	186
16L	8.9	2.2	1.4	25.5	189	179	178	180	173	169	175	180	183
16R	7.5	2.1	0.9	18.1	198	191	181	171	170	167	178	175	182
17L	8.1	2.0	0.7	16.2	183	172	170	180	165	165	169	172	174
17R	8.4	2.5	0.5	27.4	195	181	177	179	174	172	190	185	189
18L	8.6	2.1	1.0	20.7	168	166	162	161	158	153	152	156	158
18R	8.0	2.4	0.7	20.2	189	181	177	174	174	171	168	167	177
19L	8.0	1.6	0.7	15.0	189	192	187	188	181	N/A	173	N/A	182
19R	8.9	2.3	0.8	18.1	195	191	179	192	180	183	186	183	190
20L	8.4	1.6	1.2	32.3	171	175	159	165	150	157	156	161	159
20R	8.1	1.7	0.8	27.0	186	186	184	187	188	188	187	178	173
21L	8.0	1.9	0.9	23.0	174	186	185	180	178	174	165	168	162
21R	9.0	2.0	0.9	28.1	189	193	183	182	181	177	172	177	181
22L	8.2	1.9	0.7	16.9	159	146	148	154	156	156	160	163	165
22R	8.4	1.9	0.7	15.6	168	169	169	167	166	162	157	161	157
23L	9.0	2.0	N/A	14.4	180	159	177	165	176	185	190	190	201
23R	9.1	2.5	1.0	21.7	187	173	180	183	184	189	196	202	203
24L	8.9	1.9	1.1	30.4	193	190	185	183	177	187	188	192	189
24R	8.7	1.8	0.8	20.2	193	186	183	180	175	179	176	179	181
25L	9.1	2.5	1.2	37.2	148	168	168	163	174	177	183	186	188
25R	8.8	1.9	1.1	26.0	187	185	186	183	178	176	170	179	186
26L	8.6	1.8	1.3	18.6	205	189	200	195	190	189	188	174	175
26R	9.5	2.0	0.7	21.1	169	166	161	171	168	171	184	187	175
27L	9.3	2.0	1.3	24.4	186	N/A	N/A	186	N/A	N/A	178	N/A	N/A

(*continued on next page*)

Table 1 (*continued*)

Ear	Cochlea Ø (mm)	BCNC Ø (mm)	CN CSA (mm^2)	IAC CSA (mm^2)	eCAP threshold (CL)								
					22	21	20	19	18	17	16	15	14
27R	8.4	2.4	1.3	25.0	207	N/A	N/A	N/A	N/A	N/A	187	N/A	N/A
28L	N/A	2.5	1.3	22.1	N/A	166	N/A	171	N/A	175	185	187	187
28R	8.6	2.0	2.0	31.2	210	N/A	N/A	198	N/A	N/A	184	N/A	N/A
29L	8.7	2.4	1.1	24.0	183	184	176	179	167	170	173	163	182
29R	7.8	2.2	0.9	21.4	174	N/A	N/A	175	N/A	N/A	167	N/A	N/A
30L	8.0	1.7	1.7	15.1	N/A	N/A	N/A	N/A	N/A	N/A	N/A	N/A	N/A
30R	7.9	1.6	0.8	22.6	N/A	N/A	N/A	N/A	N/A	N/A	N/A	N/A	N/A
31L	8.5	2.3	0.9	36.6	174	N/A	N/A	170	N/A	N/A	163	N/A	N/A
31R	8.4	2.1	1.3	16.0	189	N/A	N/A	177	N/A	N/A	174	N/A	N/A
32L	8.3	1.6	1.1	20.5	174	N/A	N/A	168	N/A	N/A	190	N/A	N/A
32R	8.7	2.6	N/A	25.0	210	178	174	N/A	178	193	206	208	201
33L	8.4	2.0	1.3	20.8	186	N/A	N/A	N/A	N/A	N/A	183	N/A	N/A
33R	8.4	2.6	1.0	23.1	210	N/A	193	196	N/A	184	N/A	N/A	N/A
34L	9.2	2.8	1.5	24.3	192	180	177	181	171	N/A	186	N/A	192
34R	9.1	2.0	1.1	21.2	192	N/A	N/A	N/A	N/A	N/A	188	N/A	N/A
35L	8.3	2.0	1.2	20.9	181	180	178	179	178	184	186	192	195
35R	9.0	2.3	0.6	14.4	177	167	173	184	169	169	178	145	164
36L	8.4	2.1	1.1	23.0	N/A	153	162	162	177	171	192	180	171
36R	9.0	1.8	0.8	26.8	204	196	192	216	210	202	226	211	224
37L	8.5	2.0	1.3	19.3	207	201	199	208	201	197	208	202	205
37R	8.0	1.8	0.8	18.9	177	175	170	179	172	169	167	167	171
38L	9.0	2.4	1.4	23.4	180	180	171	174	174	179	185	186	191
38R	8.2	2.1	0.9	36.6	201	N/A	N/A	187	N/A	N/A	194	N/A	N/A
39L	8.3	2.1	1.5	33.6	201	N/A	188	188	N/A	187	204	N/A	201
39R	8.1	1.9	N/A	16.0	177	181	176	169	160	167	164	171	177
40L	7.8	1.7	1.2	34.2	198	190	186	183	187	184	202	186	192
40R	8.1	2.0	1.1	N/A	192	183	177	190	172	170	191	175	174
41L	8.9	2.3	1.5	9.9	204	197	194	192	186	189	196	200	202
41R	7.8	1.9	0.7	14.4	183	173	172	178	181	188	201	202	201
42L	8.6	2.2	0.8	26.0	162	163	169	171	165	168	179	181	188
42R	7.9	2.2	1.0	17.2	198	199	191	181	180	171	173	169	175
43L	8.1	2.0	1.1	15.3	177	170	166	168	159	160	169	169	167
43R	8.4	2.3	1.5	29.7	189	182	172	184	182	177	190	188	196
44L	8.8	2.1	0.8	18.9	165	168	169	165	167	161	181	176	181
44R	8.2	2.4	1.3	23.1	186	178	173	183	171	162	172	166	164
45L	8.0	1.6	1.7	16.3	168	163	174	172	170	191	186	196	193
45R	8.9	2.3	0.3	21.2	111	148	159	178	178	169	171	176	186
46L	8.4	1.7	1.5	33.1	159	159	163	158	164	155	142	152	155
46R	8.2	1.7	2.3	28.6	N/A	N/A	N/A	N/A	N/A	N/A	N/A	N/A	N/A
47L	7.9	2.1	0.9	25.4	198	188	188	186	185	181	195	175	170
47R	8.9	2.1	1.2	30.8	210	202	198	194	189	187	187	201	207
48L	8.2	1.7	N/A	18.1	162	145	146	159	166	172	184	171	161
48R	8.4	1.6	0.7	13.7	168	161	157	163	157	168	174	180	190
49L	9.3	1.7	1.4	14.4	171	153	163	180	180	191	193	195	146
49R	8.8	2.7	1.0	25.2	187	186	189	194	188	192	195	204	205
50L	8.9	2.1	1.2	31.2	160	145	177	184	182	178	182	177	188
50R	8.5	1.9	1.4	20.2	145	144	165	165	163	166	160	175	183
51L	8.9	2.9	1.2	32.5	187	174	159	179	173	177	180	192	197
51R	8.9	2.1	1.3	24.4	181	152	168	187	182	174	161	170	172
52L	8.5	1.9	N/A	22.4	202	190	193	191	189	192	190	191	197
52R	9.5	2.3	N/A	17.2	154	146	147	183	184	N/A	192	188	122
Mean	8.5	2.1	1.05	23.0	185	176	176	181	176	177	183	181	183
Ear	**eCAP threshold (CL)**												
	13	**12**	**11**	**10**	**9**	**8**	**7**	**6**	**5**	**4**	**3**	**2**	**1**
1L	184	N/A	196	N/A	N/A	204	N/A	199	N/A	N/A	194	N/A	193
1R	196	N/A	197	N/A	N/A	209	N/A	211	N/A	N/A	217	N/A	199
2L	193	188	193	192	188	184	178	176	183	182	198	208	N/A
2R	191	N/A	201	N/A	N/A	213	N/A	215	N/A	N/A	195	N/A	190
3L	195	197	204	206	212	210	207	201	202	201	199	202	196
3R	161	N/A	170	N/A	N/A	189	N/A	190	N/A	N/A	194	N/A	160
4L	N/A	N/A	N/A	N/A	N/A	N/A	N/A	N/A	N/A	N/A	N/A	N/A	N/A
4R	N/A	N/A	N/A	N/A	N/A	N/A	N/A	N/A	N/A	N/A	N/A	N/A	N/A
5L	195	N/A	204	N/A	N/A	203	N/A	207	N/A	N/A	197	N/A	214
5R	196	N/A	198	N/A	N/A	207	N/A	207	N/A	N/A	197	N/A	214
6L	189	N/A	204	N/A	N/A	226	N/A	219	N/A	N/A	186	N/A	202
6R	210	208	217	211	215	212	210	211	203	193	187	183	208
7L	N/A	N/A	206	N/A	N/A	N/A	N/A	220	N/A	N/A	N/A	N/A	226
7R	197	N/A	207	N/A	N/A	218	N/A	219	N/A	N/A	202	N/A	193
8L	213	N/A	205	N/A	N/A	190	N/A	182	N/A	N/A	178	N/A	205
8R	208	N/A	216	N/A	N/A	221	N/A	219	N/A	N/A	208	N/A	214
9L	189	192	193	198	196	201	198	206	193	189	188	188	199
9R	N/A	N/A	N/A	N/A	N/A	N/A	N/A	N/A	N/A	N/A	N/A	N/A	N/A
10L	216	201	204	135	156	222	222	234	216	207	216	210	225

(*continued on next page*)

Table 1 (*continued*)

Ear	Cochlea Ø (mm)	BCNC Ø (mm)	CN CSA (mm^2)	IAC CSA (mm^2)	eCAP threshold (CL)								
					22	21	20	19	18	17	16	15	14
10R	214	214	218	219	219	227	225	227	226	223	229	218	229
11L	196	194	196	201	210	216	212	218	208	208	210	207	208
11R	177	179	192	187	191	198	182	201	189	187	187	175	166
12L	196	197	209	204	208	197	200	201	197	196	206	208	208
12R	196	N/A	201	N/A	N/A	190	N/A	196	N/A	N/A	186	N/A	208
13L	196	N/A	203	N/A	N/A	213	N/A	203	N/A	N/A	198	N/A	183
13R	197	190	200	203	168	201	204	206	198	194	195	201	211
14L	194	178	196	193	201	216	209	219	208	207	212	207	205
14R	179	183	185	197	201	208	206	208	212	207	210	205	211
15L	212	215	217	217	221	226	222	221	218	212	205	212	217
15R	202	192	205	182	175	224	219	225	210	213	223	202	214
16L	191	200	195	203	204	203	202	198	204	141	196	196	193
16R	183	185	186	190	193	191	191	189	188	185	181	183	184
17L	176	181	184	150	125	181	145	107	181	175	159	163	202
17R	201	199	207	204	198	215	199	210	201	189	199	188	199
18L	165	171	182	191	193	202	199	200	198	194	194	189	193
18R	180	184	187	192	195	198	198	195	195	193	190	191	190
19L	194	193	202	209	208	215	188	182	109	105	168	180	208
19R	185	193	199	201	201	206	173	199	201	195	196	191	196
20L	160	159	162	145	171	179	175	175	189	196	192	188	187
20R	169	161	169	173	182	188	186	194	202	203	197	196	187
21L	163	176	175	189	195	171	183	212	213	211	208	204	168
21R	189	199	195	215	221	228	232	234	227	218	222	224	217
22L	167	175	176	184	191	193	197	199	199	197	198	195	190
22R	161	165	162	176	183	188	195	195	204	200	179	212	208
23L	201	200	197	184	192	215	183	190	182	190	152	194	175
23R	210	207	208	208	205	202	203	201	186	192	186	172	173
24L	198	199	199	197	193	192	186	190	190	195	197	207	215
24R	209	211	205	212	217	213	194	196	216	216	212	200	191
25L	194	195	201	195	156	195	184	188	182	179	181	181	191
25R	184	189	198	201	202	197	202	200	206	204	205	206	218
26L	176	176	156	211	211	211	209	212	210	212	206	207	200
26R	192	194	212	215	199	190	209	214	212	214	212	217	215
27L	200	N/A	198	N/A	N/A	213	N/A	207	N/A	N/A	199	N/A	202
27R	N/A	N/A	200	N/A	N/A	N/A	N/A	163	N/A	N/A	N/A	N/A	202
28L	192	192	184	187	182	183	180	180	186	185	196	204	216
28R	199	N/A	198	N/A	N/A	221	N/A	210	N/A	N/A	201	N/A	214
29L	185	189	192	203	207	205	199	172	190	189	188	191	193
29R	158	N/A	159	N/A	N/A	176	N/A	187	N/A	N/A	178	N/A	184
30L	N/A	N/A	N/A	N/A	N/A	N/A	N/A	N/A	N/A	N/A	N/A	N/A	N/A
30R	N/A	N/A	N/A	N/A	N/A	N/A	N/A	N/A	N/A	N/A	N/A	N/A	N/A
31L	181	N/A	192	N/A	N/A	199	N/A	192	N/A	N/A	175	N/A	172
31R	191	N/A	186	N/A	N/A	195	N/A	205	N/A	N/A	200	N/A	211
32L	189	N/A	203	N/A	N/A	218	N/A	217	N/A	N/A	199	N/A	199
32R	N/A	207	205	205	203	215	203	200	198	194	194	183	187
33L	N/A	N/A	201	N/A	N/A	N/A	N/A	N/A	N/A	N/A	N/A	N/A	226
33R	175	N/A	207	N/A	N/A	205	N/A	206	N/A	N/A	N/A	N/A	196
34L	208	203	207	201	198	205	199	197	189	185	186	186	202
34R	N/A	N/A	201	N/A	N/A	N/A	N/A	205	N/A	N/A	N/A	N/A	202
35L	196	207	201	208	202	198	197	190	192	184	186	211	212
35R	188	186	189	187	123	193	189	189	180	187	188	194	211
36L	192	150	204	204	147	219	207	213	198	186	198	198	216
36R	233	222	232	221	226	240	228	244	227	226	233	220	229
37L	221	217	224	225	230	237	232	244	224	231	236	232	238
37R	176	173	186	187	179	197	193	199	194	192	196	142	187
38L	197	201	204	205	203	N/A	195	N/A	199	195	193	195	196
38R	201	N/A	210	N/A	N/A	202	N/A	209	N/A	N/A	204	N/A	199
39L	204	209	213	N/A	N/A	215	N/A	204	N/A	N/A	197	N/A	211
39R	178	186	186	199	204	208	210	211	205	197	193	194	199
40L	236	194	192	196	199	215	206	219	201	198	217	193	208
40R	192	182	201	202	201	218	212	223	209	210	220	206	220
41L	209	213	216	217	210	220	219	216	217	216	219	217	220
41R	213	214	220	206	202	224	203	221	199	198	216	229	N/A
42L	192	198	209	171	125	189	199	214	196	193	199	191	211
42R	180	179	183	191	191	208	202	199	190	185	176	178	184
43L	187	179	188	192	195	198	197	194	197	199	201	201	205
43R	198	200	207	204	204	210	202	204	200	199	199	191	193
44L	189	191	204	202	204	202	196	194	197	192	195	192	199
44R	172	174	186	187	193	196	196	207	193	158	186	186	184
45L	191	196	194	198	207	204	206	104	193	143	162	196	205
45R	184	189	187	190	192	189	195	194	195	188	192	187	193
46L	156	158	165	167	173	180	185	189	192	194	195	192	193
46R	N/A	N/A	N/A	N/A	N/A	N/A	224	226	221	222	239	217	216
47L	165	165	162	156	184	148	124	177	185	185	179	185	184

(*continued on next page*)

Table 1 (*continued*)

Ear	Cochlea Ø (mm)	BCNC Ø (mm)	CN CSA (mm^2)	IAC CSA (mm^2)	eCAP threshold (CL)								
					22	21	20	19	18	17	16	15	14
47R	212	217	227	233	238	238	220	229	221	216	221	217	235
48L	170	167	174	179	183	187	195	195	201	199	200	202	202
48R	193	200	205	212	218	219	214	213	214	206	200	207	220
49L	134	105	182	196	166	174	182	157	140	176	162	189	220
49R	209	213	212	210	212	210	204	201	201	198	195	196	188
50L	190	195	199	198	194	194	192	194	192	188	198	200	200
50R	166	157	194	207	187	109	178	227	215	218	198	193	191
51L	196	199	206	212	210	206	203	198	199	199	193	192	188
51R	181	187	198	197	207	202	203	209	208	205	196	181	170
52L	195	207	212	217	214	209	213	209	212	206	207	206	209
52R	130	166	212	205	215	196	168	168	174	216	226	217	218
Mean	190	190	197	197	195	203	199	202	199	196	198	198	202

References

[1] S.J. Dettman, D. Pinder, R.J.S. Briggs, R.C. Dowell, J.R. Leigh, Communication development in children who receive the cochlear implant younger than 12 Months: risks versus benefits, Ear Hear. 28 (2) (Apr. 2007) 11S–18S, https://doi.org/10.1097/AUD.0b013e31803153f8.

[2] C.A. Buchman, et al., Cochlear implantation in children with labyrinthine anomalies and cochlear nerve deficiency: implications for auditory brainstem implantation: CI in Inner Ear Malformations, Laryngoscope 121 (9) (Sep. 2011) 1979–1988, https://doi.org/10.1002/lary.22032.

[3] C.S. Birman, J.A. Brew, W.P.R. Gibson, E.J. Elliott, CHARGE syndrome and Cochlear implantation: difficulties and outcomes in the paediatric population, Int. J. Pediatr. Otorhinolaryngol. 79 (4) (Apr. 2015) 487–492, https://doi.org/10.1016/j.ijporl.2015.01.004.

[4] H. Kim, D.Y. Kim, E.J. Ha, H.Y. Park, Clinical value of measurement of internal auditory canal in pediatric cochlear implantation, Ann. Otol. Rhinol. Laryngol. 128 (6_suppl) (Jun. 2019) 61S–68S, https://doi.org/10.1177/0003489419835234.

[5] A. Alballaa, et al., Incomplete partition type III revisited—long-term results following cochlear implant, HNO 68 (S1) (Jan. 2020) 25–32, https://doi.org/10.1007/s00106-019-00732-z.

[6] W.K. Lai, N. Dillier, A simple two-component model of the electrically evoked compound action potential in the human cochlea, Audiol. Neurotol. 5 (6) (2000) 333–345, https://doi.org/10.1159/000013899.

[7] W.K. Lai, N. Dillier, Comparing neural response telemetry amplitude growth functions with loudness growth functions: preliminary results, Ear Hear. 28 (2) (Apr. 2007) 42S–45S, https://doi.org/10.1097/AUD.0b013e3180315104.

[8] C.A. Miller, C.J. Brown, P.J. Abbas, S.-L. Chi, The clinical application of potentials evoked from the peripheral auditory system, Hear. Res. 242 (1–2) (Aug. 2008) 184–197, https://doi.org/10.1016/j.heares.2008.04.005.

[9] E.K. Jeon, C.J. Brown, C.P. Etler, S. O'Brien, L.-K. Chiou, P.J. Abbas, Comparison of electrically evoked compound action potential thresholds and loudness estimates for the stimuli used to program the advanced bionics cochlear implant, J. Am. Acad. Audiol. 21 (1) (2010) 16–27, https://doi.org/10.3766/jaaa.21.1.3. Jan.

[10] S. Han, L. Wang, D. Zhang, K. Peng, Neural response telemetry thresholds in patients with cochlear nerve canal stenosis, Otolaryngol. Neck Surg. 153 (3) (Sep. 2015) 447–451, https://doi.org/10.1177/0194599815592365.

[11] J.H. Jang, et al., Can radiological measurements of cochlear nerve parameters predict cochlear implant outcome? Our experience in 87 ears, Clin. Otolaryngol. 44 (6) (Nov. 2019) 1142–1146, https://doi.org/10.1111/coa.13419.

[12] S. He, et al., Responsiveness of the electrically stimulated cochlear nerve in children with cochlear nerve deficiency, Ear Hear. 39 (2) (2018) 238–250, https://doi.org/10.1097/AUD.0000000000000467.

[13] T. Morita, Y. Naito, J. Tsuji, T. Nakamura, S. Yamaguchi, J. Ito, Relationship between cochlear implant outcome and the diameter of the cochlear nerve depicted on MRI, Acta Otolaryngol. 124 (sup551) (Feb. 2004) 56–59, https://doi.org/10.1080/03655230310016708.

[14] S. Söderqvist, S. Lamminmäki, A. Aarnisalo, T. Hirvonen, S.T. Sinkkonen, V. Sivonen, Intraoperative transimpedance and spread of excitation profile correlations with a lateral-wall cochlear implant electrode array, Hear. Res. 405 (Jun. 2021), 108235, https://doi.org/10.1016/j.heares.2021.108235.

[15] F. Venail, et al., Modeling of auditory neuron response thresholds with cochlear implants, BioMed Res. Int. (2015) 1–10, https://doi.org/10.1155/2015/394687, 2015.

[16] K.N. Jahn, J.G. Arenberg, Electrophysiological estimates of the electrode–neuron interface differ between younger and older listeners with cochlear implants, Ear Hear. 41 (4) (Jul. 2020) 948–960, https://doi.org/10.1097/AUD.0000000000000827.

[17] G. Alexiades, A. Dhanasingh, C. Jolly, Method to estimate the complete and two-turn cochlear duct length, Otol. Neurotol. 36 (5) (Jun. 2015) 904–907, https://doi.org/10.1097/MAO.0000000000000620.

[18] K. Chetcuti, S. Kumbla, The internal acoustic canal - another review area in paediatric sensorineural hearing loss, Pediatr. Radiol. 46 (4) (Apr. 2016) 562–569, https://doi.org/10.1007/s00247-015-3496-4.

[19] B. Herman, S. Angeli, Differences in cochlear nerve cross-sectional area between normal hearing and postlingually deafened patients on MRI, Otolaryngol. Neck Surg. 144 (1) (Jan. 2011) 64–66, https://doi.org/10.1177/0194599810390884.

[20] B. Escudé, C. James, O. Deguine, N. Cochard, E. Eter, B. Fraysse, The size of the cochlea and predictions of insertion depth angles for cochlear implant electrodes, Audiol. Neurotol. 11 (1) (2006) 27–33, https://doi.org/10.1159/000095611.

[21] S.-I. Hatsushika, R.K. Shepherd, Y.C. Tong, G.M. Clark, S. Funasaka, Dimensions of the scala tympani in the human and cat with reference to cochlear implants, Ann. Otol. Rhinol. Laryngol. 99 (11) (Nov. 1990) 871–876, https://doi.org/10.1177/000348949009901104.

[22] G.K.A. van Wermeskerken, A.F. van Olphen, K. Graamans, Imaging of electrode position in relation to electrode functioning after cochlear implantation, Eur. Arch. Oto-Rhino-Laryngol. 266 (10) (Oct. 2009) 1527–1531, https://doi.org/10.1007/s00405-009-0939-2.

[23] C.J. Long, et al., Examining the electro-neural interface of cochlear implant users using psychophysics, CT scans, and speech understanding, J. Assoc. Res. Otolaryngol. 15 (2) (Apr. 2014) 293–304, https://doi.org/10.1007/s10162-013-0437-5.

[24] A. Mewes, G. Brademann, M. Hey, Comparison of perimodiolar electrodes: imaging and electrophysiological outcomes, Otol. Neurotol. 41 (7) (Aug. 2020) e934–e944, https://doi.org/10.1097/MAO.0000000000002790.

[25] S. Biedron, A. Prescher, J. Ilgner, M. Westhofen, The internal dimensions of the cochlear scalae with special reference to cochlear electrode insertion trauma, Otol. Neurotol. 31 (5) (Jul. 2010) 731–737, https://doi.org/10.1097/MAO.0b013e3181d27b5e.

[26] F.B. van der Beek, J.J. Briaire, K.S. van der Marel, B.M. Verbist, J.H.M. Frijns, Intracochlear position of cochlear implants determined using CT scanning versus fitting levels: higher threshold levels at basal turn, Audiol. Neurotol. 21 (1) (2016) 54–67, https://doi.org/10.1159/000442513.

[27] S. Anne, et al., Utility of intraoperative and postoperative radiographs in pediatric cochlear implant surgery, Int. J. Pediatr. Otorhinolaryngol. 99 (Aug. 2017) 44–48, https://doi.org/10.1016/j.ijporl.2017.05.018.

[28] R. Nakamichi, et al., Establishing normal diameter range of the cochlear and facial nerves with 3D-CISS at 3T, Magn. Reson. Med. Sci. 12 (4) (2013) 241–247, https://doi.org/10.2463/mrms.2013-0004.

[29] V. Vincenti, F. Ormitti, E. Ventura, M. Guida, A. Piccinini, E. Pasanisi, Cochlear implantation in children with cochlear nerve deficiency, Int. J. Pediatr. Otorhinolaryngol. 78 (6) (Jun. 2014) 912–917, https://doi.org/10.1016/j.ijporl.2014.03.003.

[30] C.S. Birman, H.R.F. Powell, W.P.R. Gibson, E.J. Elliott, Cochlear implant outcomes in cochlea nerve aplasia and hypoplasia, Otol. Neurotol. 37 (5) (Jun. 2016) 438–445, https://doi.org/10.1097/MAO.0000000000000997.

[31] K.A. Gordon, B.C. Papsin, R.V. Harrison, Toward a battery of behavioral and objective measures to achieve optimal cochlear implant stimulation levels in children, Ear Hear. 25 (5) (Oct. 2004) 447–463, https://doi.org/10.1097/01.aud.0000146178.84065.b3.

[32] L.M. Telmesani, N.M. Said, Electrically evoked compound action potential (ECAP) in cochlear implant children: changes in auditory nerve response in first year of cochlear implant use, Int. J. Pediatr. Otorhinolaryngol. 82 (Mar. 2016) 28–33, https://doi.org/10.1016/j.ijporl.2015.12.027.

[33] F. Christov, M.B. Gluth, S. Hans, S. Lang, D. Arweiler-Harbeck, Impact of cochlear tonotopy on electrically evoked compound action potentials (ECAPs), Acta Otolaryngol. 139 (1) (Jan. 2019) 22–26, https://doi.org/10.1080/00016489.2018.1533993.

[34] A. Franke-Trieger, D. Mürbe, Estimation of insertion depth angle based on cochlea diameter and linear insertion depth: a prediction tool for the CI422, Eur. Arch. Oto-Rhino-Laryngol. 272 (11) (Nov. 2015) 3193–3199, https://doi.org/10.1007/s00405-014-3352-4.

[35] E. Erixon, H. Rask-Andersen, How to predict cochlear length before cochlear implantation surgery, Acta Otolaryngol. 133 (12) (Dec. 2013) 1258–1265, https://doi.org/10.3109/00016489.2013.831475.

[36] P. Mittmann, et al., Radiological and NRT-ratio–based estimation of Slim Straight cochlear implant electrode positions: a multicenter study, Ann. Otol. Rhinol.

Laryngol. 126 (1) (Jan. 2017) 73–78, https://doi.org/10.1177/0003489416675355.